Geophysical Research Letters

RESEARCH LETTER
10.1029/2018GL079780

On the Statistical Distribution of Total Water in Cirrus Clouds

B. Kärcher[1], T. Thornberry[2], M. Krämer[3], and E. J. Jensen[4]

[1]Deutsches Zentrum für Luft- und Raumfahrt, Institut für Physik der Atmosphäre, Oberpfaffenhofen, Germany, [2]National Oceanic and Atmospheric Administration, Earth System Research Laboratories, and University of Colorado Boulder, Cooperative Institute for Research in Environmental Sciences, Boulder, CO, USA, [3]Forschungszentrum Jülich, Institut für Energie und Klimaforschung, Jülich, Germany, [4]National Aeronautics and Space Administration, Ames Research Center, Moffett Field, CA, USA

Key Points:
- We analyze aircraft measurements of total water distributions in cirrus clouds
- We develop an observation-based parameterization of cirrus total water distributions
- We find that the susceptibility of distribution skewness to changes in ice content is small

Correspondence to:
B. Kärcher,
bernd.kaercher@dlr.de

Citation:
Kärcher, B., Thornberry, T. D., Krämer, M., & Jensen, E. J. (2018). On the statistical distribution of total water in cirrus clouds. *Geophysical Research Letters*, *45*. https://doi.org/10.1029/2018GL079780

Received 26 JUL 2018
Accepted 2 SEP 2018
Accepted article online 5 SEP 2018

Abstract Distributions of total water in cirrus provide important information on cloud-scale variability. Observations of water variables in cirrus are sparse, limiting our ability to constrain factors controlling their evolution and lifetimes. We present and analyze aircraft measurements of tropical and extratropical cirrus total water statistics. We show that observed distributions are replicated by a parametric model that only requires knowledge of in-cloud temperatures. We parameterize the temporal decay of cloud ice content and distribution skewness forced by ice crystal sedimentation and find that ice water content decays at a much faster rate than skewness in the absence of cloud ice and skewness sources. The sensitivity of skewness to changes in ice water content is small. Our methodology and findings may prove useful for studies addressing statistical cloud schemes and cirrus life cycles.

Plain Language Summary Probability distributions are important modeling tools to describe the atmospheric effects of clouds. This study reports distributions of total (gas plus ice phase) water in high tropospheric ice clouds (cirrus) obtained from measurements with research aircraft in tropical, midlatitude, and Arctic locations. We make a first attempt to base the origin of the distributions on physical processes and to reconstruct them with a statistical approach based on knowledge of cloud temperatures. We thereby show that the observed, heavy tails of the total water statistics are linked to the presence of cloud ice crystals. While cloud ice mass diminishes by ice crystal settling, the tails decay at a much slower rate. We hope that our methodology proves to be useful in support of studies analyzing cirrus life cycles.

1. Introduction

The need to parameterize clouds and their effects in low-resolution (large-scale) weather prediction and climate models is well recognized (Randall et al., 2007). One way to tackle the cloud parameterization issue is to assign a probability density function (PDF) to total water concentrations in atmospheric regions containing clouds. Besides providing cloud fraction and cloud mass, the functional forms of total water statistics contain information on cloud-scale variability that is otherwise absent in low-resolution models. The variability underlying such PDFs is caused by unresolved microphysical and dynamical processes. Low-order PDF moments (mean, variance, and skewness) are used to establish links between water variables (cloud microphysics), cloud fraction (macrophysics), and cloud-controlling factors (e.g., dynamical forcing mechanisms) on the one hand and to derive consistent estimates of variables describing the effects of clouds (e.g., radiative fluxes) on the other.

Relationships among water variables in tropospheric clouds on horizontal scales of some tens of kilometers have been studied using aircraft data (Wood & Field, 2000) and large-domain cloud-resolving model simulations (Tompkins, 2002). These studies clearly show that humidity, temperature, and cloud variables exhibit significant spatial variability on the scale of grid cells in regional and global models, violating assumptions made in some model cloud schemes that represent clouds by water variables averaged over a grid cell. Physical mechanisms, controlling factors of, and relationships among, cloud variables must be well understood in order to safely employ PDF-based (statistical) cloud schemes across all cloud types. Linking PDF moments to cloud microphysical processes is challenging (Klein et al., 2005; Larson & Golaz, 2005; Quaas, 2012; Tompkins, 2008). Improving statistical cloud schemes is particularly challenging for cirrus (Kärcher, 2017).

While total water PDFs representative for a grid cell of a low-resolution model may include cloud-free regions, focusing on in-cloud PDFs is useful for process interpretation and cloud life cycle analyses. Arguably, the latter are more challenging for cirrus than for liquid-phase clouds, as cirrus form in situ at relative humidities substantially (many tens of percent) above ice saturation (Koop et al., 2000) and dissolve completely only at much lower (several tens of percent) values below saturation (Ström et al., 2003). Long water phase relaxation times in cirrus blur cloud boundaries and emphasize the continuum aspect of aerosol/cirrus systems (Kärcher & Solomon, 1999).

Here we present an approach to construct cirrus total water PDFs from their constituent water vapor and cloud ice statistics and confront this methodology with in situ observations. Moreover, we study the link between the skewness of the total water statistic and the settling of cloud ice into warmer and drier air, which constitutes an irreversible sink for total water in cirrus. In this way, we quantify microphysically forced skewness decay in support of efforts to advance statistical cloud schemes regarding ice phase processes. We describe the observational basis in section 2, outline how cirrus total water statistics are modeled, compare results with in situ measurements of water variables in tropical cirrus, and carry out the skewness analysis in section 3. Section 4 concludes our study.

2. Aircraft Measurements

The Airborne Tropical Tropopause Experiment deployment from Guam (13°N) in 2014 provided extensive measurements of cold (mainly <200 K) cirrus in the tropical tropopause layer (TTL; Jensen, Pfister, et al., 2017). Flights with the National Aeronautics and Space Administration Global Hawk aircraft profiled extensively between about 14 and 18 km over the western Pacific. The aircraft spent more than 30 hr in cirrus clouds, with instruments measuring temperature, water vapor, and cloud microphysical properties (Woods et al., 2018). The cirrus clouds sampled were primarily formed in situ in the TTL well away from deep convective systems. The Airborne Tropical Tropopause Experiment water vapor and total water measurements included here were made using the National Oceanic and Atmospheric Administration water instrument, a two-channel tunable diode laser-based hygrometer (Thornberry et al., 2015).

Temperature, water vapor, and cirrus cloud microphysical properties were measured in the Arctic winter on board the Russian aircraft Geophysica during the European Polar Stratospheric Cloud and Lee Wave Experiment combined with the European Space Agency's Environmental Satellite validation experiment in 2003. All Arctic flights were made from Kiruna in northern Sweden (68°N). Midlatitude observations were performed aboard a Learjet during the CIRRUS campaigns in 2003, 2004, and 2006 from Hohn, Germany (54°N; Krämer et al., 2009; Schiller et al., 2008). Total water and water vapor were measured using the Lyman-α photofragment fluorescence hygrometers Fast In-situ Stratospheric Hygrometer (Meyer et al., 2015) and Fluorescent Airborne Stratospheric Hygrometer (Khaykin et al., 2013), respectively. Data taken in middle- and high-latitude cirrus have been merged into an extratropical data set to obtain a sample size large enough for robust statistical evaluation.

3. Results and Discussion

3.1. Total Water Statistics

To build total water statistics for pure ice clouds, we consider three water variables in terms of mass mixing ratios: vapor (q_v), cloud ice (q_i), and total water ($q_t = q_v + q_i$). We view PDF(q_t) as a joint probability density of its vapor and cloud ice parts:

$$\mathrm{PDF}(q_t) = \int \mathrm{d}q_v \, \mathrm{PDF}(q_v) \, \mathrm{PDF}(q_i = q_t - q_v) \, . \tag{1}$$

As illustrated in Figure 1, we make the assumption that the presence of cloud ice constrains q_v locally to ice saturation, that is, $q_v \simeq q_s$. This does not hold during short-term ice formation events (Kärcher & Jensen, 2017). For the purpose of this study, we identify the vapor PDF with a delta distribution:

$$\mathrm{PDF}(q_v) = \delta(q_v - q_s(T)) \, . \tag{2}$$

In stark contrast to liquid-phase clouds, water vapor mixing ratios within cirrus may depart significantly from q_s: ice nucleation from supercooled aerosol particles (those with the highest freezing thresholds) occurs

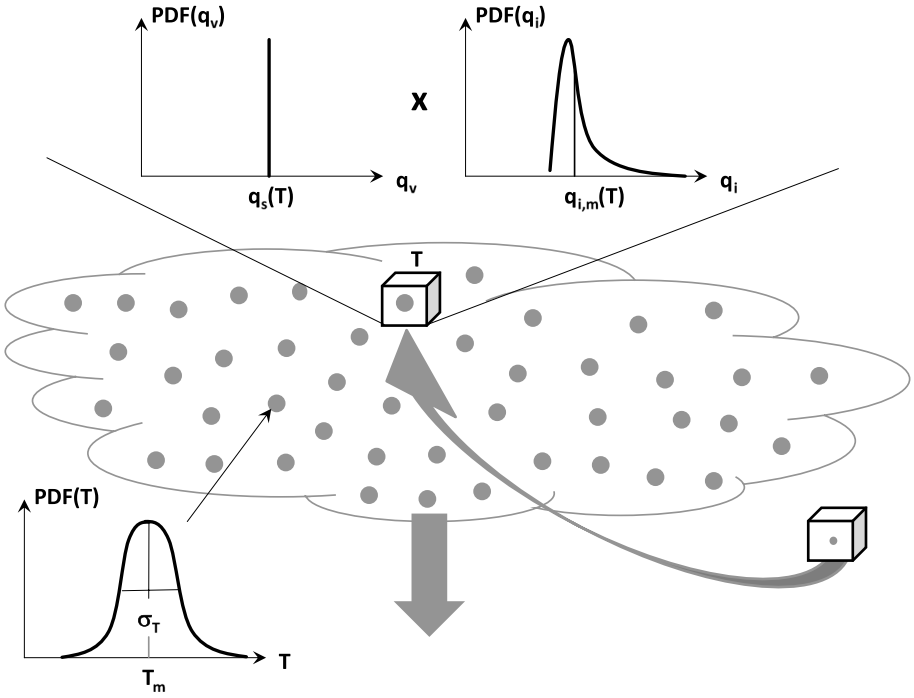

Figure 1. Schematic illustrating our methodology to build a total water PDF representing cirrus. The PDF is formulated in terms of water mass mixing ratios, q, and decomposed into a vapor distribution, PDF(q_v), and a cloud ice distribution, PDF(q_i). The cloud area is characterized by a temperature distribution, PDF(T). The Lagrangian history (curved arrow) of each cloudy parcel (box) and microphysical processes including ice crystal formation and sedimentation determine local q_i values. Water vapor deposition and sublimation processes leave q_t invariant but dampen cloud-scale supersaturation fluctuations causing q_v to stay near the local ice saturated value, $q_s(T)$. Gravitational settling of ice crystals (vertical arrow) constitutes an irreversible loss of cloud ice. PDF = probability density function.

within 1.5–1.7q_s (Koop et al., 2000) and ice crystals can survive conditions as dry as 0.6q_s (Ström et al., 2003). However, aircraft studies show that the majority of relative humidities measured inside many cirrus types tend to be near ice saturation (Jensen, Thornberry, et al., 2017; Krämer et al., 2009; Ovarlez et al., 2002). Local vapor-ice thermodynamic equilibrium is attained at time scales that decrease in proportion to the integral radius, defined as the product of the ice crystal number density and the mean ice crystal size (Korolev & Mazin, 2003). Except in cirrus regions with small integral radii, vapor-ice equilibrium is established rapidly (within 10 min; Kärcher et al., 2014). Equilibration times for deviations from ice saturation can become considerably longer (up to 2 hr) for thin TTL cirrus (Jensen et al., 2013; Rollins et al., 2016). Steady state ice supersaturation may be accounted for in equation (2) by replacing $q_s \rightarrow fq_s$ with $f > 1$; here we fix $f = 1$.

We assume that in-cloud temperatures are normally distributed with a mean value, T_m, and standard deviation, σ_T:

$$\mathrm{PDF}(T) = \frac{1}{\sqrt{2\pi}\sigma_T} \exp\left[-\frac{1}{2}\left(\frac{T - T_m}{\sigma_T}\right)^2\right]. \tag{3}$$

While temperature fluctuations within cirrus may be caused by gravity wave activity, variability in T, embodied in σ_T, can also be generated by radiative heating and cooling, generating small-scale convection, predominantly in optically thick cirrus.

While knowledge of the in-cloud temperature distribution supposedly suffices to estimate PDF(q_v) as suggested above, this is in principle not longer the case for PDF(q_i). The ice content in every cloud element is determined by its supersaturation history and associated microphysical processes including ice nucleation, growth, sublimation, and sedimentation (Figure 1). Therefore, we expect a distribution of cloud ice amount at any given T. Such variability is seen in in situ observations that also suggest that mean cloud ice mass concentrations in nonconvective cirrus correlate well with local T (Luebke et al., 2013; Schiller et al., 2008). With decreasing T, less water vapor is available for deposition and mean cloud ice content decreases.

Given T, we model the cloud ice statistic as a Gamma distribution:

$$\mathrm{PDF}(q_i) = \frac{\lambda^{\mu+1}}{\Gamma(\mu+1)}\, q_i^{\mu}\, \exp(-\lambda q_i)\,, \quad \lambda = \frac{\mu+1}{q_{i,m}(T)} \tag{4}$$

with the temperature-dependent scale parameter λ, the shape parameter, μ, and the Gamma function, $\Gamma(x)$. Parameterizations for mean, nonconvective cloud ice mixing ratios for midlatitude and Arctic cirrus and for tropical cirrus, $q_{i,m}(T)$, are taken from Schiller et al. (2008; their Table 2). We fix $\mu = 1/3$ and note that the sensitivity of $\mathrm{PDF}(q_t)$ to this parameter is small.

Introducing the temperature statistic, $\mathrm{PDF}(T)$, carrying out the integration over q_v and another over T transforms equation (1) into

$$\mathrm{PDF}(q_t; T_m, \sigma_T, \mu) = \mathcal{N}_t \int \mathrm{d}T\, \mathrm{PDF}(T)\, \mathrm{PDF}(q_i = q_t - q_s(T), T)\,, \tag{5}$$

with a normalization constant, $\mathcal{N}_t$. Equation (5) assumes that in a cloud element at temperature T, the vapor stays at ice saturation and the probability to find an ice content q_i, constrained by q_t, is distributed around the mean value, $q_{i,m}(T)$. The total water statistic from this model is unimodal. Its skewness depends on how different $\mathrm{PDF}(q_i)$ are superimposed and can only be evaluated numerically.

To judge the realism of this approach, we compare in Figure 2 modeled $\mathrm{PDF}(q_t)$ to those of nonconvective cirrus observed in tropical and extratropical regions (section 2). While the model tends to underestimate the high q_t tails, the shapes of the unimodal distributions are very well replicated. In both cases, q_v is the dominant contribution to q_t near $q_{t,m}$. However, this may not be a universal feature of $\mathrm{PDF}(q_t)$, rather the partitioning between vapor and cloud ice amount will be a function of cloud age. For instance, initial cloud ice mass is typically large in convectively generated anvil cirrus (e.g., Figure 8 in Schiller et al., 2008) but will diminish over time due to sedimentation. Moreover, q_i dominates q_t at high q_t values and is therefore mainly responsible for the heavy tail of $\mathrm{PDF}(q_t)$. For this reason, we expect a tight relation between the distribution skewness and cloud ice settling, hence q_i.

Potential problems affecting the data-model comparison include (i) the width, σ_T, of $\mathrm{PDF}(T)$ and (ii) parameterized $q_{i,m}$ values. Concerning (i), using the observed σ_T values in equation (3) worsens the agreement between observed and modeled $\mathrm{PDF}(q_t)$, which is why we regard σ_T as a fit parameter for this comparison. The fitted σ_T values deviate from those directly obtained from the data (tropical: 1.45 K; extratropical: 0.63 K). This difference is small (0.25 K) for the tropical cirrus case but significant (0.87 K) for the extratropical cirrus containing larger ice crystals. This suggests that factors other than temperature also contribute to vapor variability, such as supersaturation changes induced by ice crystal sedimentation. Regarding (ii), if $q_{i,m}(T)$ does not capture actual mean ice water contents (IWCs) well, different parameterizations could be applied, for example, modeled tails of $\mathrm{PDF}(q_t)$ increase by enhancing $q_{i,m}$.

Observed $\mathrm{PDF}(q_i)$ are reasonably well approximated by Gamma distributions. The instrumental detection limit is apparent in the tropical case due to overall lower q_i values. Some in situ measurements indicate that cirrus q_i statistics exhibit bimodality, with a second mode appearing at the low q_i tail of $\mathrm{PDF}(q_i)$ (Luebke et al., 2013). While it is interesting to develop a deeper understanding of how microphysical processes act together to shape these distributions and disentangle this impact from the impact of data sampling, such subtle deviations from the assumed unimodal $\mathrm{PDF}(q_i)$ at the lowest q_i values do not affect $\mathrm{PDF}(q_t)$ much.

We recall that our model has not been designed to provide a best fit to aircraft data but rather to build confidence in the understanding of processes affecting total water variability in cirrus. This said, the agreement between predicted and observed total water statistics, in particular the PDF shape, is very encouraging. We continue studying how the distribution tail evolves with time when affected by ice crystal sedimentation.

3.2. Ice Microphysics

The mass mixing ratio of cloud ice is related to IWC via $\mathrm{IWC} = \varrho q_i$, the mass of cloud ice per unit volume of air. Here $\varrho(p, T)$ is the mass density of air, and p is the air pressure. A simple budget equation for IWC takes the form

$$\frac{\mathrm{dIWC}}{\mathrm{d}t} = P - L, \quad L = \frac{\mathrm{IWC}}{\tau}, \quad \tau = \frac{(\Delta z/2)}{V}, \tag{6}$$

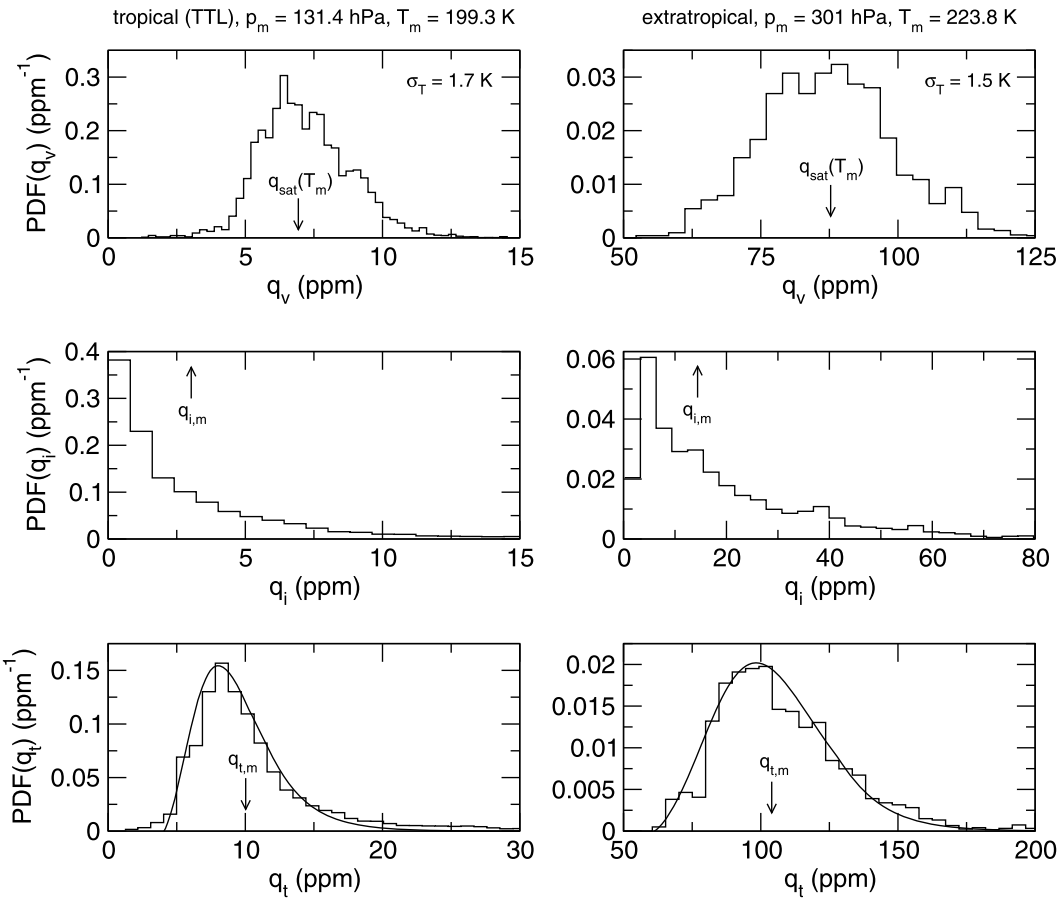

Figure 2. Probability density functions of (top row) water vapor, (middle row) cloud ice, and (bottom row) total water content in nonconvective cirrus sampled with aircraft at (left column) low latitudes and (right column) middle latitudes and the Arctic. Shown are in-cloud PDFs derived from the measurements (stepped curves) and total water PDFs from the model (solid). Measured temperatures were sampled within 197–202 K (tropical cirrus) and 222–226 K (extratropical), leading to the mean values of pressure and temperature used to constrain the model PDFs as indicated; measured mean mass mixing ratios of water variables are also indicated. All PDFs are normalized to unity. Standard deviations used to evaluate the model temperature statistics are estimated such that the resulting ice saturated water vapor statistics match the observed PDFs. TTL = tropical tropopause layer; PDF = probability density function.

where P and L denote source and loss terms for IWC, respectively. We assume that the level of supersaturation is low enough to prevent ice nucleation from occurring and changes in IWC by depositional growth are small ($P = 0$), consistent with the cloud staying close to thermal equilibrium. The IWC loss term is determined by ice crystal settling out of the cloud layer into ice-subsaturated air, Δz is a measure of the vertical cloud depth, V is the particle sedimentation velocity—interpreted as a mass-weighted terminal fall speed of a size-dispersed population of cirrus ice crystals, and τ is the characteristic time scale of irreversible loss of ice water due to sedimentation. IWC is assumed to be homogeneously distributed in the layer, so the average distance ice crystals must settle before being removed is $\Delta z/2$. To parameterize V for an ice crystal ensemble, we follow Heymsfield (2003) and choose the power law dependence:

$$V = a \cdot \mathrm{IWC}^b \equiv V_\star \left(\frac{\mathrm{IWC}}{\mathrm{IWC}_\star} \right)^b , \tag{7}$$

with coefficients a and b varying across cirrus types. To estimate L, we use $b = 0.24$, $\mathrm{IWC}_\star = 10\,\mathrm{mg/m^3}$, and $V_\star = 55$ cm/s for a relationship that approximates in situ measurements across tropical and midlatitude ice clouds (Figure 11c in Heymsfield, 2003). More detailed parameterizations of V are available (e.g., Mitchell et al., 2011), but their application requires knowledge of ice crystal size and habit distributions, which are not available for most measurements considered here.

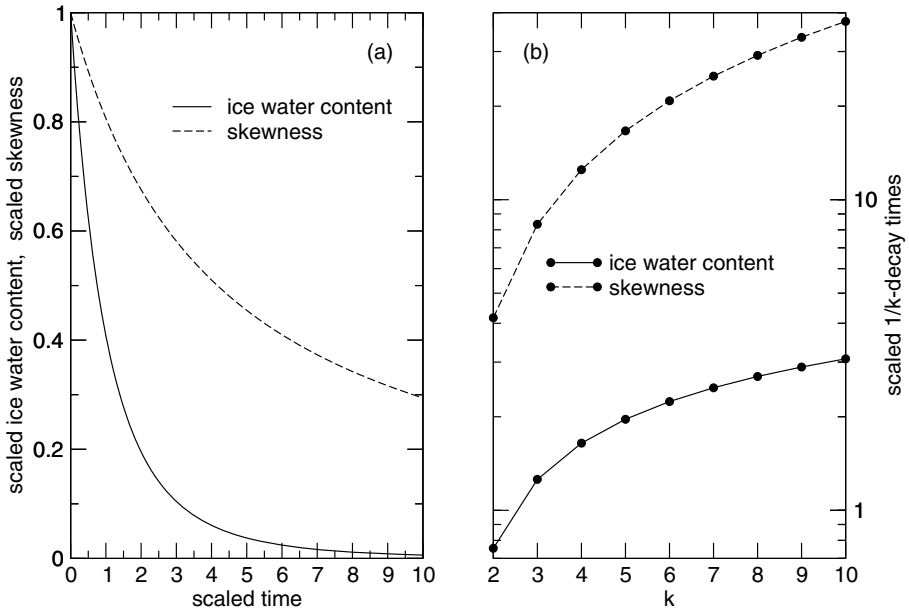

Figure 3. (a) Normalized ice water content, IWC/IWC$_0$, and skewness, $\varsigma(t)/\varsigma_0$, versus scaled time, $(t-t_0)/\tau_0$, evaluated with a fall speed parameter b=0.24. (b) The respective normalized $1/k$ decay times, $t_{1/k}^{\mathrm{IWC}}/\tau_0$ and $t_{1/k}^{\varsigma}/\tau_0$, as a function of k. Initial time scales τ_0 range between about 0.25–0.5 hr for Δz=1 km, depending on T according to Table 1.

It is instructive to quantify typical values for P and L. In a series of cloud-resolving model simulations, Köhler (1999) injected cloud ice over several hours into a Δz = 2-km-thick layer at rates P = (40–200) ppm/hr to simulate anvil cirrus formation. Using equation (7) with the parameters given above leads to a sedimentation loss time scale $\tau_\star = (\Delta z/2)/V_\star \simeq 0.5$ hr. We estimate $L < 200$ ppm/hr, roughly in line with the cloud simulations that indicate the buildup of q_i values up to 100 ppm in the cloud layer. At later stages in the absence of cloud ice production, L decreases as IWC diminishes.

3.3. Skewness Relaxation Due to Sedimentation

Prognostic equations for higher-order PDF(q_t) moments better constrain total water PDFs in statistical cloud schemes and help remove empiricism in their mathematical formulation (Schemann, 2014). Convective detrainment of frozen liquid cloud water producing upper level anvil cirrus increases the skewness of PDF(q_t) (Tompkins, 2002). The same may happen after in situ ice crystal nucleation and subsequent depositional growth, but likely to a smaller degree, since aerosol particles have a small liquid water content. Skewness diminishes due to settling of cloud ice, small-scale horizontal mixing and turbulent dissipation, and large-scale subsidence forcing cloud dissolution.

In the absence of a skewness (ς) source, we parameterize the temporal evolution of ς due to sedimentation as a Newtonian relaxation:

$$\frac{\mathrm{d}\varsigma}{\mathrm{d}t} = -\frac{\varsigma}{\tau}\,, \quad \tau(t) = \frac{\tau_0}{(\mathrm{IWC}(t)/\mathrm{IWC}_0)^b}\,, \quad \tau_0 = \frac{(\Delta z/2)}{a\cdot \mathrm{IWC}_0^b}\,, \tag{8}$$

with the time-dependent IWC loss time scale τ taken from equations (6) and (7), since we regard the sedimentation loss of IWC as the only factor affecting skewness decay. Initial values of IWC and ς have a subscript 0. We focus on part of an ice cloud's life cycle between times t_0 and t, where $P = 0$ and assume that it evolves in a uniform environment, that is, $\Delta z, p, T$ = const. In a more comprehensive description of skewness decay, in which IWC changes are evaluated consistently with supersaturation, the associated total loss rate is defined as the sum of τ^{-1} values from all loss sources.

The corresponding solution of equations (6) and (7) reads

$$\frac{\mathrm{IWC}(t)}{\mathrm{IWC}_0} = \frac{1}{[1 + b(t-t_0)/\tau_0]^{1/b}}\,. \tag{9}$$

Table 1
Characteristic Time Scales Describing IWC and ς Decay Stages for a Range of Air Temperatures, T

T (K)	p (mb)	IWC (mg/m^3)	V (km/hr)	$t^{\varsigma}_{1/2}$ (hr)	$t^{\mathrm{IWC}}_{1/2}$ (hr)	$t^{\varsigma}_{1/10}$ (hr)	$t^{\mathrm{IWC}}_{1/10}$ (hr)
200	179	0.60	1.00	2.09	0.38	18.80	1.54
205	195	1.14	1.17	1.79	0.33	16.07	1.32
210	212	1.98	1.33	1.57	0.29	14.07	1.16
215	231	3.19	1.50	1.40	0.25	12.54	1.03
220	250	4.83	1.65	1.26	0.23	11.36	0.93
225	270	6.90	1.80	1.16	0.21	10.42	0.86
230	292	9.42	1.94	1.08	0.20	9.67	0.80
235	315	12.36	2.07	1.01	0.18	9.06	0.75
240	339	15.66	2.19	0.95	0.17	8.56	0.70

Note. Air pressure, p, varies adiabatically with T. Initial values for mean ice water content, IWC, and ensemble fall speeds, $V \propto \mathrm{IWC}^b$ (using b=0.24), are also given. Mean IWC values represent nonconvective cirrus probed in aircraft measurements. Time scales are evaluated for Δz=1 km and scale $\propto \Delta z$.

The temporal decay of IWC is slower than exponential, since τ increases with diminishing IWC. Inserting equation (9) into equation (8) leads to

$$\frac{\varsigma(t)}{\varsigma_0} = \frac{1}{1 + b(t - t_0)/\tau_0}\,. \tag{10}$$

The times over which IWC and ς decay to $1/k$ of their initial values are given by ($k > 1$):

$$t^{\mathrm{IWC}}_{1/k} = \tau_0 \frac{k^b - 1}{b}\,, \quad t^{\varsigma}_{1/k} = \tau_0 \frac{k - 1}{b}\,. \tag{11}$$

Equations (9) and (10) are displayed in Figure 3. IWC diminishes within few hours, potentially allowing supersaturation to increase and thereby ice crystal nucleation to occur within the cloud area, prolonging the cloud's life time. By contrast, skewness decays considerably more slowly, leading to much larger decay times, especially for large k (in aged cirrus).

We list in Table 1 the times $t_{1/k}$ for $k = 2$ and $k = 10$ characterizing short-term and long-term stages of decay, respectively. These results confirm that signatures of skewness may be seen for many hours and that IWC decays considerably faster than ς, by a factor $(k^b - 1)/(k - 1)$; see equation (11). The $t_{1/k}$ values exhibit a marked temperature dependence via IWC_0 that enters the initial IWC loss rate due to sedimentation, $1/\tau_0$; see equation (8).

According to equation (7), $V = a\mathrm{IWC}^b$, and a tenfold increase in IWC increases V only by a factor of $10^b = 1.7$. This insensitivity of the ice crystal ensemble fall speed to the IWC is caused by the low value of the parameter b, which does not vary much (Heymsfield, 2003). In the idealized case of a monodisperse population of spherical particles, $b = 2/3$, equation (7) reverts to Stokes' exact solution for fall speeds of spheres in a viscous flow (Lamb & Verlinde, 2011), if the parameter a is properly chosen. In this case, the sensitivity (susceptibility) of V to changes in IWC would be larger.

Combining equations (9) and (10) eliminates the time dependence and allows the decaying skewness of PDF(q_t) to be diagnosed as a function of IWC or V:

$$\frac{\varsigma}{\varsigma_0} = \left(\frac{\mathrm{IWC}}{\mathrm{IWC}_0}\right)^b = \frac{V}{V_0}\,. \tag{12}$$

This relationship connects a bulk cloud property and the power law parameter related to the terminal fall speed of the ice crystal population to the skewness of the total water statistic. An immediate implication of equation (12) is that the susceptibility of skewness to changes in IWC, $\mathrm{d}\ln(\varsigma)/\mathrm{d}\ln(IWC) = b$, is small. According to the above, we expect the susceptibility to be larger in thin cirrus clouds prevalent at the tropical tropopause, since they contain a large fraction of quasi-spheroidal ice crystals (Woods et al., 2018), implying larger b.

4. Summary and Outlook

In this study, we analyzed for the first time probability distributions of total water within cirrus clouds based on aircraft measurements. To parameterize the effect of clouds on temperature and moisture fields and the radiation balance, statistical cloud schemes link physical processes to such distributions. However, it is generally difficult to formulate microphysical source and sink terms for higher distribution moments such as variance and skewness. Observations presumably face considerable challenges in capturing high-order moments of total water distributions, as large amounts of data are required for accurate and statistically robust evaluation of PDF tail extremities.

We devised a model to parameterize such distributions based on knowledge of in-cloud temperatures alone and demonstrated its performance by comparing its results with in situ data. We specified the effect of ice crystal sedimentation on the skewness of cirrus total water statistics. Provided in the form of a sink term affecting the temporal evolution of distribution skewness, this result may prove useful for advancing statistical cloud schemes, as it provides a link between a crucial microphysical process affecting cirrus (cloud ice settling) and an important macrophysical model variable (cloud fractional coverage) in a physically consistent manner.

By studying characteristic decay times for IWC and total water distribution skewness due to ice crystal sedimentation in the absence of associated production terms, we conclude that cirrus IWC typically decays more than fivefold faster than skewness. The time scale analysis suggests that sedimentation is an important ice cloud dissipation mechanism, rapidly diminishing the ice content within few hours. We expect this to hold in the presence of ice crystal depositional growth in aging cirrus, which increases cloud ice content and therefore enhances the efficiency of sedimentation losses relative to an unforced cloud. In the absence of ice growth, sedimentation becomes less efficient over time because ice crystals with smaller mean sizes have lower fall speeds. This manifests itself in sedimentation loss time scales that increase over time. The consequences of the interplay between deposition growth and sedimentation for the lifetime of high ice clouds, including the possibility of new ice formation, remain to be explored. Our methodology may be extended to include effects of ice nucleation and growth, making it a useful tool for observation- and model-based cirrus life cycle analyses.

Acknowledgments
This work was supported by NASA's ATTREX project. Data used in this study are openly available on espoarchive.nasa.gov and in Schiller et al. (2008) cited in the reference list. We thank Tina Jurkat for thoughtful comments on the first manuscript draft.

References

Heymsfield, A. J. (2003). Properties of tropical and midlatitude ice cloud particle ensembles. Part II: Applications for mesoscale and climate models. *Journal of the Atmospheric Sciences*, *60*, 2592–2611.

Jensen, E. J., Diskin, G., Lawson, R. P., Lance, S., Bui, T. P., Hlavka, D., et al. (2013). Ice nucleation and dehydration in the tropical tropopause layer. *Proceedings of the National Academy of Sciences of the United States of America*, *110*, 2041–2046. https://doi.org/10.1073/pnas.1217104110

Jensen, E. J., Pfister, L., Jordan, D. E., Bui, T. P., Ueyama, R., Singh, H. B., et al. (2017). The NASA Airborne Tropical Experiment. High-altitude aircraft measurements in the tropical western Pacific. *Bulletin of the American Meteorological Society*, *98*, 129–143. https://doi.org/10.1175/BAMS-D-14-00263.1

Jensen, E. J., Thornberry, T. D., Rollins, A. W., Ueyama, R., Pfister, L., Bui, T., et al. (2017). Physical processes controlling the spatial distributions of relative humidity in the tropical tropopause layer over the Pacific. *Journal of Geophysical Research: Atmospheres*, *122*, 6094–6107. https://doi.org/10.1002/2017JD026632

Kärcher, B. (2017). Cirrus clouds and their response to anthropogenic activities. *Current Climate Change Reports*, *3*, 45–57. https://doi.org/10.1007/s40641-017-0060-3

Kärcher, B., Dörnbrack, A., & Sölch, I. (2014). Supersaturation variability and cirrus ice crystal size distributions. *Journal of the Atmospheric Sciences*, *71*, 2905–2926.

Kärcher, B., & Jensen, E. J. (2017). Microscale characteristics of homogeneous freezing events in cirrus clouds. *Geophysical Research Letters*, *44*, 2027–2034. https://doi.org/10.1002/2016GL072486

Kärcher, B., & Solomon, S. (1999). On the composition and optical extinction of particles in the tropopause region. *Journal of Geophysical Research*, *104*, 27,441–27,459.

Khaykin, S. M., Engel, I., Vömel, H., Formanyuk, I. M., Kivi, R., Korshunov, L. I., et al. (2013). Arctic stratospheric dehydration—Part 1: Unprecedented observation of vertical redistribution of water. *Atmospheric Chemistry and Physics*, *13*, 11,503–11,517.

Klein, S. A., Pincus, R., Hannay, C., & Xu, K.-M. (2005). Coupling a statistical scheme to a mass flux scheme? *Journal of Geophysical Research*, *110*, D15S06. https://doi.org/10.1029/2004JD005017

Köhler, M. (1999). *Explicit prediction of ice clouds in general circulation models* (pp. 167). Los Angeles: Dissertation, University of California.

Koop, T., Luo, B. P., Tsias, A., & Peter, T. (2000). Water activity as the determinant for homogeneous ice nucleation in aqueous solutions. *Nature*, *601*, 611–614.

Korolev, A. V., & Mazin, I. P. (2003). Supersaturation of water vapor in clouds. *Journal of the Atmospheric Sciences*, *60*, 2957–2974.

Krämer, M., Schiller, C., Afchine, A., Bauer, R., Gensch, I., Mangold, A., et al. (2009). Ice supersaturations and cirrus cloud crystal numbers. *Atmospheric Chemistry and Physics*, *9*, 3505–3522.

Lamb, D., & Verlinde, J. (2011). *Physics and Chemistry of Clouds*. Cambridge, UK: Cambridge University Press.

Larson, V. E., & Golaz, J.-C. (2005). Using probability density functions to derive consistent closure relationships among higher-order moments. *Monthly Weather Review*, *133*, 1023–1042.

Luebke, A. E., Avallone, L. M., Schiller, C., Meyer, J., Rolf, C., & Kraemer, M. (2013). Ice water content of Arctic, midlatitude, and tropical cirrus - Part 2: Extension of the database and new statistical analysis. *Atmospheric Chemistry and Physics*, *13*, 6447–6459.

Meyer, J., Rolf, C., Schiller, C., Rohs, S., Spelten, N., Afchine, A., et al. (2015). Two decades of water vapor measurements with the FISH fluorescence hygrometer: a review. *Atmospheric Chemistry and Physics*, *15*, 8521–8538.

Mitchell, D. L., Mishra, S., & Lawson, R. P. (2011). Representing the ice fall speed in climate models: Results from Tropical Composition, Cloud and Climate Coupling (TC4) and the Indirect and Semi-Direct Aerosol Campaign (ISDAC). *Journal of Geophysical Research*, *116*, D00T03. https://doi.org/10.1029/2010JD015433

Ovarlez, J., Gayet, J.-F., Gierens, K., Ström, J., Ovarlez, H., & Auriol, F. (2002). Water vapour measurements inside cirrus clouds in Northern and Southern hemispheres during INCA. *Geophysical Research Letters*, *29*(16), 1813. https://doi.org/10.1029/2001GL014440

Quaas, J. (2012). Evaluating the "critical relative humidity" as a measure of subgrid-scale variability of humidity in general circulation model cloud cover parameterizations using satellite data. *Journal of Geophysical Research*, *117*, D09208. https://doi.org/10.1029/2012JD017495

Randall, D. A., Wood, R. A., Bony, S., Colman, R., Fichefet, T., Fyfe, J., et al. (2007). *Climate models and their evaluation*.

Rollins, A. W., Thornberry, T. D., Gao, R. S., Woods, S., Lawson, R. P., Bui, T. P., et al. (2016). Observational constraints on the efficiency of dehydration mechanisms in the tropical tropopause layer. *Geophysical Research Letters*, *43*, 2912–2918. https://doi.org/10.1002/2016GL067972

Schemann, V. (2014). *Towards a scale aware cloud process parameterization for global climate models* (pp. 137). Hamburg: Reports on Earth System Science 145, Max-Planck-Institut für Meteorologie.

Schiller, C., Krämer, M., Afchine, A., Spelten, N., & Sitnikov, N. (2008). Ice water content of Arctic, midlatitude, and tropical cirrus. *Journal of Geophysical Research*, *113*, D24208. https://doi.org/10.1029/2008JD010342

Ström, J., Seifert, M., Kärcher, B., Ovarlez, J., Minikin, A., Gayet, J.-F., et al. (2003). Cirrus cloud occurrence as function of ambient relative humidity: a comparison of observations obtained during the INCA experiment. *Atmospheric Chemistry and Physics*, *3*, 1807–1816.

Thornberry, T. D., Rollins, A. W., Gao, R. S., Watts, L. A., Ciciora, S. J., McLaughlin, R. J., et al. (2015). A two-channel, tunable diode laser-based hygrometer for measurement of water vapor and cirrus cloud ice water content in the upper troposphere and lower stratosphere. *Atmospheric Measurement Techniques*, *8*, 211–224.

Tompkins, A. M. (2002). A prognostic parameterization for the subgrid-scale variability of water vapor and clouds in large-scale models and its use to diagnose cloud cover. *Journal of the Atmospheric Sciences*, *59*, 1917–1942.

Tompkins A. M. (2008). Cloud parametrization, *ECMWF seminar on parametrization of subgrid physical processes* (pp. 27–62). Reading, UK: European Centre for Medium-Range Weather Forecasts.

Wood, R., & Field, P. R. (2000). Relationship between total water, condensed water, and cloud fraction in stratiform clouds examined using aircraft data. *Journal of the Atmospheric Sciences*, *57*, 1888–1905.

Woods, S., Lawson, R. P., Jensen, E., Bui, T. P., Thornberry, T., Rollins, A., et al. (2018). Microphysical properties of tropical tropopause layer cirrus. *Journal of Geophysical Research: Atmospheres*, *123*, 6053–6069. https://doi.org/10.1029/2017JD028068